International Society for Rock Mechanics and Rock Engineering
Norwegian Group for Rock Mechanics

ISRM International Symposium
Eurock 2025 – Expanding the Underground Space
Trondheim, Norway, 16-20 June
ISBN 978-82-8208-079-8

Calibration of 2D Finite Element Models using Pre-Yield Axial Testing Data for Fully Grouted Rebar Rockbolts

C.P. Fischer & M.S. Diederichs
Department of Geological Sciences and Geological Engineering, Queen's University, Kingston, Canada
caitlin.fischer@queensu.ca

B. Forbes
BGC Engineering Inc., Kingston, Canada

Abstract

Built-in numerical rockbolt models are available to practitioners conducting underground excavation design using modern numerical modelling software. The ability to predict remaining support capacity against load-, strain-, or displacement-based limits relies on the ability of the numerical rockbolt model to accurately simulate rockbolt loading and deformation behaviour.

In this research, fully grouted rebar rockbolts are modelled at laboratory- and tunnel-scale using the 2D Finite Element Method (FEM) program RS2. Two rockbolt models are compared and calibrated to laboratory-scale, pre-yield, rockbolt pull testing data from distributed fiber optic strain sensing. Bolt models include a "Fully Bonded" model that is coupled with infinite stiffness to the rockmass, and a "Swellex/Split Set" model (termed the "Elasto-Plastic Interface model" in this paper) that applies a deformable interface between the rockbolt and the rockmass. Rockbolt models are assigned input parameters from manufacturer specifications and literature review to assess pre-yield rockbolt model load development and deformation. To improve bolt model performance, the bond shear stiffness (B.S.S.) parameter in the Elasto-Plastic Interface model is then calibrated.

The calibrated Elasto-Plastic Interface model is then implemented at tunnel-scale to verify rockbolt displacement and loading behaviour generated in interaction with discrete loading features. The calibrated model simulates fully grouted rebar rockbolt behaviour well at tunnel-scale, as exemplified through comparison to in-situ fiber-optic CT-bolt strain measurements. Realistic rockbolt load development lengths, shear stress distributions, and overlapping influence zones are generated by the calibrated model.

It is recommended to model fully grouted rebar rockbolts in RS2 using the Elasto-Plastic Interface model with a calibrated B.S.S. to simulate fully grouted rebar rockbolt loading and deformation behaviour. The calibrated B.S.S. value (5850 MN/m/m) in this work is significantly higher than B.S.S. values computed from the literature, but is necessary to simulate fully grouted rockbolt behaviour using the RS2 Elasto-Plastic Interface model formulation.

Keywords

Fully Grouted Rebar Rockbolts, Axial Pull Testing, Rockbolt Numerical Modelling, Finite Element Method

ISRM

NBG

1 Introduction

Grouted rebar rockbolts are widely used in civil and mining engineering to control rockmass displacements and improve excavation stability through functioning principles of rock reinforcement and holding (e.g., Farmer 1975; Hoek 2007). Grouted rebar rockbolts restrain rock deformation as they are loaded in-situ by continuous and discontinuous rock movements (e.g., Dight 1982; Hyett et al. 1996; Li and Stillborg 1999; Grasselli 2005).

1.1 Objectives and Scope

This research aims to practically and accurately model fully grouted rebar rockbolt behaviour using the 2D Finite Element Method (FEM) program RS2 by Rocscience, selected due to program accessibility and popularity in hard rock modelling. Two rockbolt models are compared to Forbes (2020a) laboratory rockbolt pull test data, using input parameters initialized based on manufacturer specifications and literature review. Bolt model performance is assessed for representativeness in terms of exponential load decay, load development, and displacement. The Elasto-Plastic Interface model is then calibrated to Forbes (2020a) laboratory rockbolt strain data. The calibrated model is implemented at tunnel-scale in interaction with discrete rockmass structure, and behaviour is compared to in-situ strain data from Forbes (2020b). Practical recommendations for the realistic modelling of fully grouted rebar rockbolts in RS2 are ultimately delivered.

1.2 Numerical Rockbolt Models

RS2 provides multiple built-in structural elements (rockbolt models) that consist of one-dimensional deformable elements that pass through the FEM mesh. RS2 rockbolts interact with modelled joints according to bolt-joint interaction theory (Rocscience technical user manuals n.d.), incorporating principles from Dight (1982) and Grasselli (2005). The RS2 rockbolt models applied in this research are described in Sections 1.2.1 and 1.2.2.

1.2.1 Fully Bonded Model

The Fully Bonded model is discretized at intersections with the FEM mesh. Each segment acts independently of others, influencing other segments only through impact on the rockmass. Axial force (F_e) in the bolt is determined from the elongation of the bolt element (Δu_e), considering bolt area (A), bolt element length (L_e), and bolt modulus (E), per Eq. (1). If axial force exceeds axial strength, bolt force is set to residual for the segment. Rock-grout and grout-bolt interfaces have infinite stiffnesses (the bolt is fully bonded to the rock, and displacement in the bolt equals that in the rock). Fully Bonded bolt discretization and axial force generation are displayed schematically in Fig. 1.

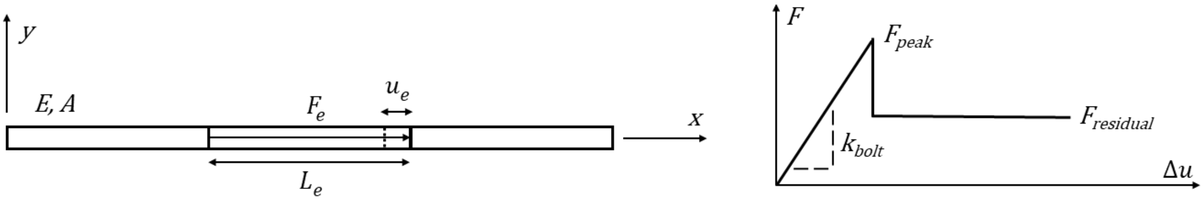

Fig. 1. Fully Bonded bolt model discretization schematic and strength criterion, after Rocscience (n.d.).

$$F_e = \frac{AE}{L_e}\Delta u_e \quad (1)$$

1.2.2 Elasto-Plastic Interface Model

The Elasto-Plastic Interface model is also discretized at intersections with the FEM mesh. Each bolt segment directly impacts neighbouring segments. Shear force develops due to relative movement between the bolt and the rockmass according to springs of assigned B.S.S. Load transfer mechanics are complex and are detailed fully in the Rocscience technical user manuals (n.d.). The bolt equilibrium equation is written per Eq. (2), where $F_{interface}$ is shear force per unit length, u_x is segment displacement, and x is segment length. Shear force develops as a linear function of relative movement between the rock (u_r) and the bolt (u_x) according to interface stiffness ($k_{interface}$) (Eq. (3)). Bolt segments are not directly connected to the element vertices and as such, a mapping procedure is used to transfer rockbolt impact to rockmass element vertices. If axial force exceeds bolt axial strength, bolt force is set to residual. Similarly, if bond strength (B.S.) is exceeded, bond force is set to residual. The title "Elasto-Plastic Interface" model is applied in this work, as residual bond strength is assigned equal to peak strength, but post-yield strengthening or weakening to a constant value may instead be applied.

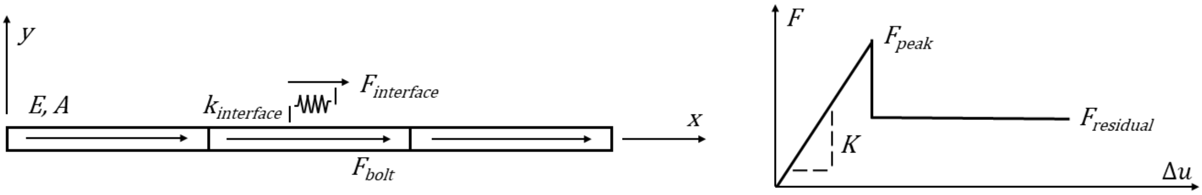

Fig. 2. Elasto-Plastic Interface bolt model discretization schematic and strength criterion, after Rocscience (n.d.). The strength criterion schematic applies separately to both the bolt shaft and the bond interface.

$$F_e = \frac{AE}{L_e} \Delta u_e \tag{2}$$

$$F_{interface} = k_{interface}(u_r - u_x) \tag{3}$$

2 Fiber-Optic Axial Testing Data

Forbes et al. (2017, 2018) developed, refined, and tested a fiber-optic instrumentation technique for rockbolts that consists of embedding and encapsulating a single mode optical fiber within shallow grooves machined along the length of a rebar shaft. The technique can measure strain at a discrete measurement interval spacing as low as 0.65 mm along a fiber optic sensor (FOS), allowing rockbolt strain profiles (i.e., nearly continuous strain measurements along the rockbolt length) to be measured. The experimental axial pull test data referenced in this research is from a 19.5 mm diameter, 1.15 m long, grouted rebar rockbolt specimen (titled “RC31-1000” in Forbes (2020a)). RC31-1000 results compare well to grouted rebar experimental results in the literature (e.g., Li et al. 2016). Forbes (2020a) test setup is shown in Fig. 3. Load is applied to the rebar free length at a displacement-controlled rate of 1 mm/min, up to 100 kN (beneath the 120 kN yield load of the rebar).

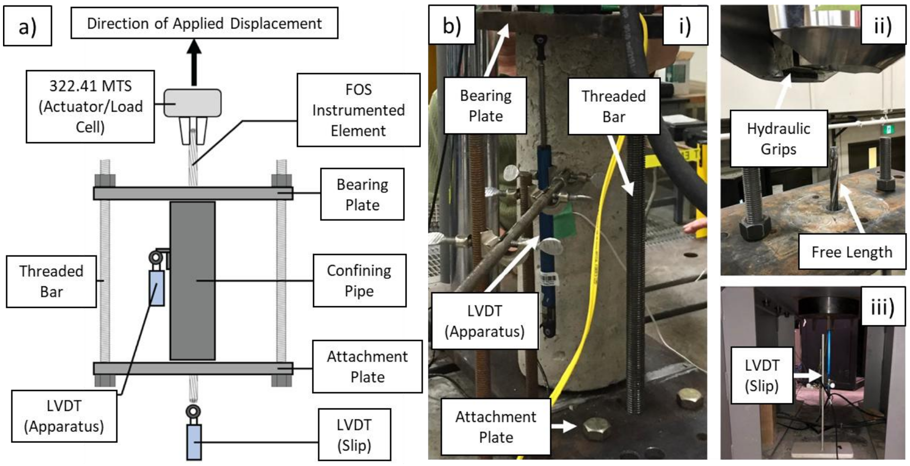

Fig. 3. Schematic and photographs of the rebar axial pull testing setup (after Forbes 2020a). The rebar is cement-grouted into a precast 31 mm center, within a 200 mm diameter concrete cylinder. The FOS is embedded within lengthwise, diametrically opposed square grooves machined along the rebar length (3.0 mm by 3.0 mm). The specimen is constrained between two steel plates, and 0.15 m of rebar free length extends through a hole in the top plate.

Axial strain is measured continuously by the FOS and is reported as an average calculated from diametrically opposing positions along the FOS to compensate for bending moment induced strain. Strains are converted to deformations (δ) per Eq. (4), by integrating axial strain along the grouted length of the test specimen, beginning at the toe end, where Δx is the spatial resolution of the FOS (0.65 mm). Axial strain is converted to axial load using Eq. (5), where A is the cross-sectional area of the rebar, and E is the Young’s Modulus of the rebar. The interfacial shear stress (τ_{int}) between the rebar and grout is calculated using Eq. (6), where r is the rebar radius and i refers to the position along the FOS at increments of Δx (Farmer 1975).

$$\delta = \int_{End\ of\ FOS\ Rebar}^{Start\ of\ FOS\ Rebar} \varepsilon_{axial}(\Delta x) \tag{4}$$

$$F_{axial} = \varepsilon_{axial} AE \tag{5}$$

$$\tau_{int} = \frac{rE}{2\Delta x}\left(\varepsilon_{axial,i+1} - \varepsilon_{axial,i-1}\right) \tag{6}$$

3 Laboratory-Scale Rockbolt Model Input Parameters

The 2D plane-strain laboratory-scale model geometry is presented in Fig. 4. The 1.15 m long rebar is oriented vertically, with its lower 1 m embedded in a concrete material (properties in Table 1), with pin boundary conditions. In RS2, rockbolt segments cannot exist outside of a defined material volume, nor can axial load be applied directly to the end of the Fully Bonded bolt model. As such, the rebar free length (0.15 m) is simulated in a low stiffness material, separated from the concrete by a low stiffness joint. Axial loading is initiated in the rockbolt using a displacement boundary condition applied to the top of the low stiffness material. Load develops uniformly in the free bolt length, thus adequately simulating behaviour. Applied displacement is increased incrementally in five stages: 0%, 25%, 50%, 75%, and 100% of final displacement required to achieve 100 kN in the bolt's loaded end.

Bolt diameter, area, steel modulus, and tensile capacity are initialized using manufacturer specifications, while B.S. and B.S.S. for the Elasto-Plastic Interface model are initialized using parameters from the literature (Table 2). Fischer et al. (2025) identified a parametric range for B.S. from approximately 0.2 to 1.1 MN/m based on a variety of pull tests (e.g., Li et al. 2016). B.S.S. in the RS2 Elasto-Plastic Interface model is defined as the slope of the elastic portion of the shear force versus shear displacement graph, expressed in the units of force/length/length. Fischer et al. (2025) estimate B.S.S. values from the literature ranging from approximately 10 to 800 MN/m/m. Specific B.S. and B.S.S. inputs applied in this work are summarized in Table 2.

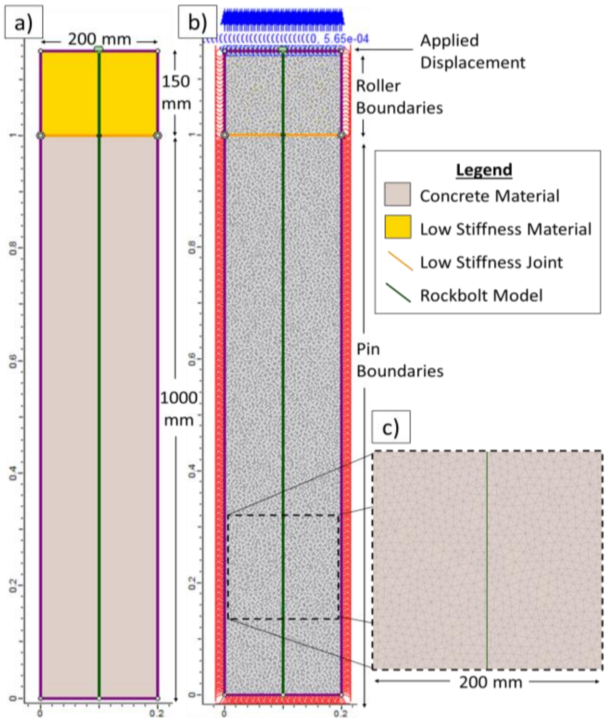

Fig. 4. RS2 model geometry after Forbes (2020a) axial pull test. a) Unmeshed, simple geometry. b) Mesh and boundary conditions, showing 10,000 uniform, six-noded mesh elements. c) Mesh inset.

Table 1. RS2 model material and joint input parameters for the Forbes (2020a) axial pull test.

Parameter	Concrete Material	Low Stiffness Material	Low Stiffness Joint
Young's Modulus (MPa)	15,600	0.001	N/A
Poisson's Ratio	0.17	0.25	N/A
Normal Stiffness (MPa/m)	N/A	N/A	0.001
Shear Stiffness (MPa/m)	N/A	N/A	0.001
Strength Model	Elastic	Elastic	Elastic

Table 2. Initial bolt model inputs for the Fully Bonded and Elasto-Plastic Interface models.

Parameter	Fully Bonded Model	Elasto-Plastic Interface Model
Bolt Diameter (mm)	19.5	19.5
Tributary Area (mm^2)	285	285
Bolt Modulus (MPa)	200,000	200,000
Tensile Capacity (MN)	0.120	0.120
Bond Strength (B.S.) (MN/m)	N/A	0.8
Bond Shear Stiffness (B.S.S.) (MN/m/m)	N/A	100

4 Laboratory-Scale Model Results

Axial load and displacement results for the Fully Bonded and Elasto-Plastic Interface models using input parameters from Table 2 are presented with the Forbes (2020a) data in Fig. 5.

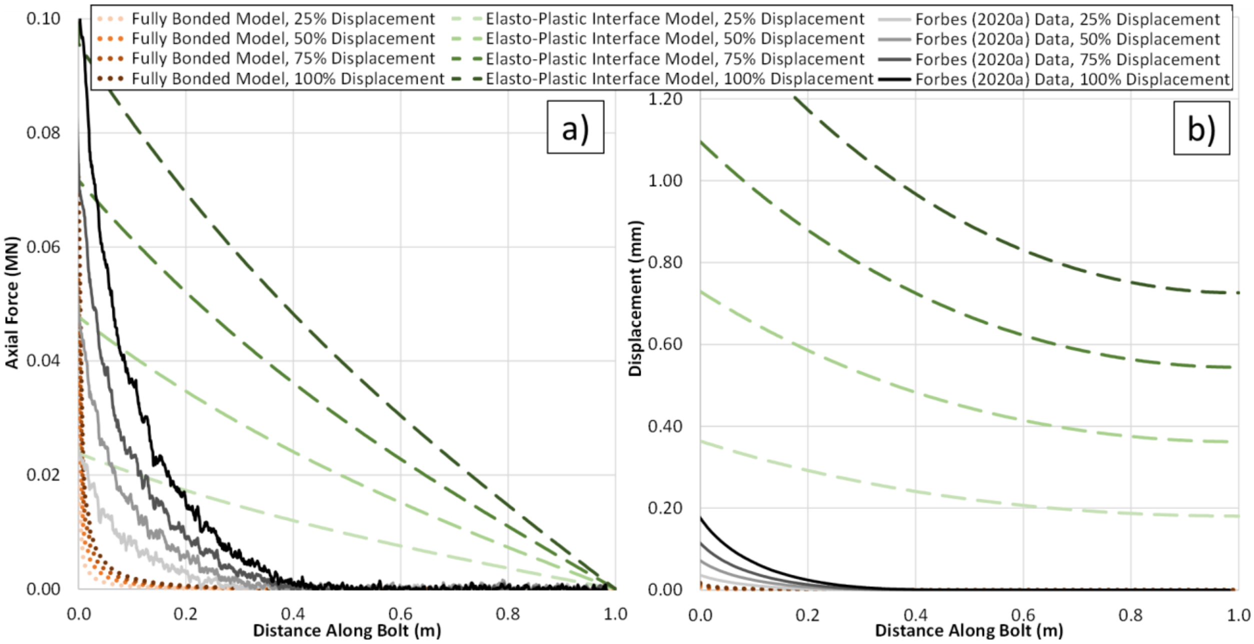

Fig. 5. a) Bolt axial load and b) bolt axial displacement for the Fully Bonded and Elasto-Plastic Interface bolt models at 25%, 50%, 75%, and 100% of final displacement to achieve 100 kN at the loaded bolt end, and the Forbes (2020a) data.

The Fully Bonded model greatly underpredicts load propagation and displacement towards the toe of the bolt compared to the Forbes (2020a) data (Fig. 5). Load decays exponentially along the bolt length (as per Farmer 1975; Li and Stillborg 1999), but decay is extremely abrupt, resulting in a load development length of 0.15 - 0.20 m compared to 0.40 - 0.45 m in the Forbes (2020a) data (corroborated by other fully grouted rebar pull test results (e.g., Li et al. 2016)). Such underpredictions occur due to the Fully Bonded model formulation, where the impact of a given bolt segment on the next is calculated through impact on the rockmass, rather than on the next bolt segment itself.

Conversely, the Elasto-Plastic Interface model greatly overpredicts load development along the bolt compared to the Forbes (2020a) data, exhibiting an unrealistic load development length of the entire bolt (1.0 m), and demonstrating limited exponential load decay. Displacement is greatly overpredicted, with the entire bolt displacing towards the pulled end (i.e., non-zero displacement at the toe end). In conclusion, both bolt models, when employing manufacturer specifications and literature-reviewed parameters, compare poorly to Forbes (2020a) experimental data.

Model calibration is therefore required to improve mechanistic performance. The B.S.S. parameter in the Elasto-Plastic Interface model is examined for calibration, as B.S. is not exceeded in pre-yield testing and therefore does not influence results. In the Fully Bonded model, no interface parameters are available for modification, and manipulating the bolt modulus has been shown to be ineffective due to the fundamental bolt model formulation (Fischer et al. 2025).

Results for the pre-yield calibrated Elasto-Plastic Interface model with a B.S.S. of 5850 MN/m/m are shown in Fig. 6. The calibrated model well represents grouted rebar behaviour in terms of load development length, exponential load decay, and displacement. The 5850 MN/m/m B.S.S. value is significantly higher than comparable values found in the literature for interface stiffness, but is required to simulate expected rockbolt displacement behaviour. The calibrated B.S.S. is program-specific and bolt model-specific, for rockbolt RC31-1000 (Forbes 2020a), but based on these results, similarly elevated B.S.S. values should be anticipated when modelling related bolt types using the RS2 Elasto-Plastic Interface model.

The RS2 Elasto-Plastic Interface model is intended for frictional rockbolts. As such, B.S.S. is a constant value calculated based on embedment length (i.e., contribution to shear force is linear). In this research, B.S.S. is used to represent mechanical interlock as well as friction for fully grouted rebar rockbolts. The use of a constant B.S.S. is a simplification, as shear stress develops non-uniformly over fully grouted rebar embedment length, which may contribute to the required elevated B.S.S. input.

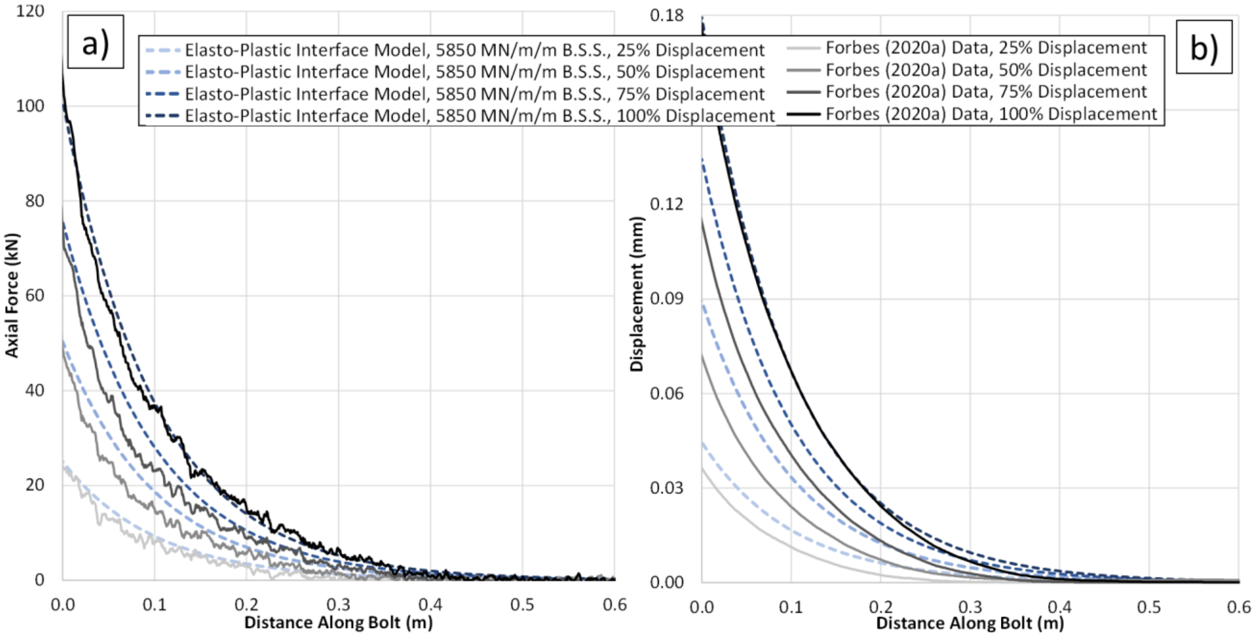

Fig. 6. a) Bolt axial load and b) bolt axial displacement for the calibrated 5850 MN/m/m B.S.S. Elasto-Plastic Interface model for 25%, 50%, 75%, and 100% of final displacement, and the Forbes (2020a) data.

5 Tunnel-Scale Rockbolt Model Input Parameters

The calibrated Elasto-Plastic Interface model (5850 MN/m/m B.S.S.) is implemented at tunnel-scale to assess model performance in interaction with discrete joints. The tunnel-scale model consists of a 10 m diameter tunnel situated at 1 km depth in an isotropic stress field in a Geological Strength Index (GSI) 65 rockmass (Hoek et al. 2002) (Fig. 7). The tunnel is excavated in five stages: the first stage is unexcavated, the second stage is excavated with 100% induced stress load applied to the tunnel boundary, and the third, fourth, and fifth stages have 40%, 5%, and 0% induced stresses applied to the excavation boundary, respectively. 5 m long rockbolts are installed in 45-degree increments around the tunnel at the face (40% support pressure) and are loaded passively. 3-noded mesh is graded denser towards the explicit rockmass zone, with an average element length of 0.25 m around the excavation. The mesh is further densified around the support element presented in this analysis (bolt B1 in the roof), with an average element length of 0.10 m along B1.

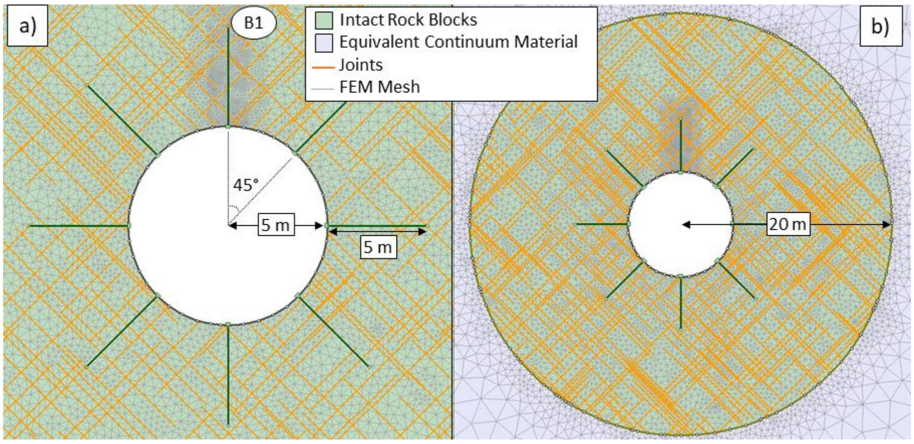

Fig. 7. a) Excavated tunnel in an explicitly modelled GSI 65 rockmass. “B1” indicates the bolt in the roof. b) Zoomed-out image of the explicit rockmass zone in the equivalent-continuum material, extending to pinned external boundaries.

The tunnel-scale model is developed using the Fischer and Diederichs (2024) methodology for explicitly modelling rockmasses of a given GSI using explicit joint networks and intact rock blocks. An elasto-plastic strength criterion is defined for the intact rock blocks using the Generalized Hoek-Brown strength criterion (Hoek et al. 2002). Joint density, 2D inclination, finite trace length, and number of joint sets are defined according to Fischer and Diederichs (2024) (Table 3).

Post-yield rockbolt model behaviour is approximated using an elasto-plastic criterion for the shaft and interface, such that the bolt may continue to deform while maintaining near-peak load prior to ultimate yield (Hoek 2007). Bond strength has been shown to follow a tri-linear failure envelope (Ren et al. 2010), which is not implementable in the RS2 bolt model. It is worth noting that in RS2, bolt yield indicators are generated at peak load, and therefore, ultimate rockbolt rupture must be assessed through manual comparison to project-specific rockbolt strain- or displacement- limits.

Table 3. Explicit rockmass model input parameters developed using the Fischer and Diederichs (2024) methodology.

Intact Rock Block Input Parameters		**Baecher Joint Network Input Parameters**	
UCS (MPa)	120	Density (joints/m)	1.0
Intact Young's Modulus, E_i (GPa)	35.0	Inclinations, 2 Sets in Plane (°)	45, -45
Unit Weight (MN/m^3)	0.027	Trace Length (m)	8.1
m_i	25	JCS (MPa)	48.8
Poisson's Ratio, v	0.25	JRC	12
GSI	85	Base Friction Angle (°)	30.3
		Normal Stiffness, K_n (MPa/m)	90,000
		Shear Stiffness, K_s (MPa/m)	22,400

6 Tunnel-Scale Model Results

Results from bolt B1 in the tunnel-scale model are demonstrated in Fig. 8. Model results are assessed compared to in-situ FOS-instrumented CT-bolt data from an active tunnel operation in the Hawkesbury Sandstone in Sydney, Australia (Forbes 2020b, not pictured). CT-bolts are a variety of fully grouted rebar rockbolt, with an added corrugated polyethylene sheath for corrosion protection. The sheath has been found to impact load development behaviour, extending load development lengths compared to conventional fully grouted rebar rockbolts.

Fig. 8 and Forbes (2020b) data both display local axial load maxima at discrete feature intersections (neutral points, per Freeman 1978). On opposing sides of a neutral point, a pickup length resists rockmass movement towards the excavation, and an anchoring length anchors the element to deeper ground. These shear stress inflections are shown by both the calibrated model (Fig. 8) and Forbes (2020b) data. Overlapping influence zones are also noted in both datasets, as expected from discrete loading features within two critical embedment lengths of one another (e.g., Hyett et al. 1996). The rockbolt model also displays realistic load development lengths at each joint (Forbes 2020a).

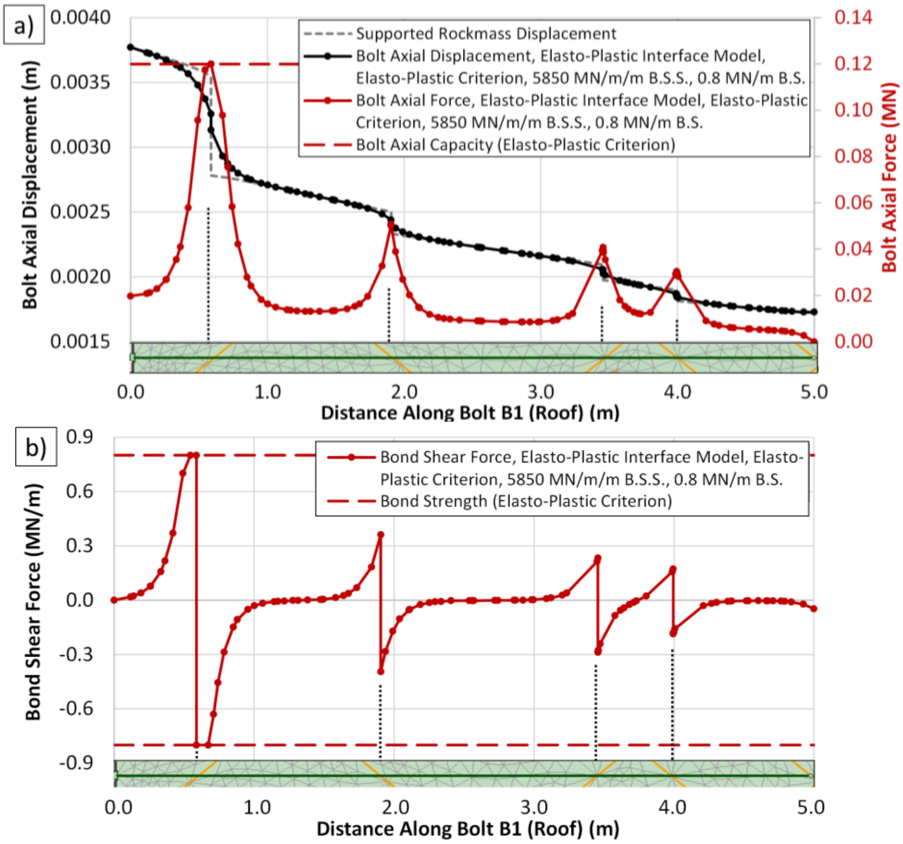

Fig. 8. a) Bolt axial displacement and bolt axial force and b) bond shear force for bolt B1 in the tunnel-scale model.

7 Conclusions

Two RS2 rockbolt model formulations (the Fully Bonded and Elasto-Plastic Interface models) are used to simulate fully grouted rebar rockbolt behaviour at laboratory- and tunnel-scale in RS2. Bolt models are first assigned input parameters from manufacturer specifications and literature review, and are compared to pre-yield fiber-optic axial pull test data from Forbes (2020a). The Fully Bonded model greatly underpredicts load development and displacement due to model formulation limitations, while the Elasto-Plastic Interface model (using initial estimates of B.S.S.) greatly overpredicts rockbolt load and displacement. Through calibration of the B.S.S. in the Elasto-Plastic Interface model, a good representation of load development and displacement is achieved. The calibrated B.S.S. of 5850 MN/m/m is significantly higher than values computed from the literature, but is required to accurately simulate fully grouted rebar behaviour using the RS2 Elasto-Plastic Interface model.

The calibrated pre-yield Elasto-Plastic Interface model is also assessed at tunnel-scale in an explicitly jointed rockmass. The calibrated rockbolt model demonstrates realistic load development lengths, neutral points, interfacial shear stress distributions, and overlapping influence zones, as discussed compared to in-situ CT-bolt data from Forbes (2020b). It is recommended that practitioners modelling fully grouted rockbolts in RS2 use the Elasto-Plastic Interface model with a calibrated B.S.S. to accurately simulate fully grouted rebar behaviour at excavation-scale, not the Fully Bonded model. Future work should include bolt models in other common geotechnical software (including 3D), other rockbolt types, considerations for shear loading, and more advanced post-yield strength formulations.

References

Dight PM (1982) Improvements to the stability of rock walls in open pit mines. Dissertation, Monash University

Farmer IW (1975) Stress distribution along a resin grouted rock anchor. International Journal of Rock Mechanics and Mining Sciences 12: 347–351

Fischer CP, Forbes B, Diederichs MS (2025) Calibration of Support Elements in 2D Finite Element Models based on Pre-Yield Axial Testing Data for Fully Grouted Rebar Rockbolts. Tunnelling and Underground Space Technology, Submitted

Fischer CP, Diederichs MS (2024) Elasto-Plastic and Post-Yield Weakening Jointed Rockmass Response in a Comparison of Equivalent-Continuum and Explicit Structural Models. Canadian Geotechnical Journal 61(4) https://doi.org/10.1139/cgj-2022-0190

Forbes B (2020a) Insight into the coaxial load distribution of fully grouted rebar, cable bolt, CT-Bolt, and D-Bolt reinforcement elements. Chapter 4, Dissertation, Queen’s University

Forbes B (2020b) Measuring the in-situ response of tunnel support using high spatial resolution optical fiber strain sensing. Chapter 6, Dissertation, Queen’s University

Forbes B, Vlachopoulos N, Hyett AJ, Diederichs MS (2017) A new optical sensing technique for monitoring shear of rock bolts. Tunnelling and Underground Space Technology 66: 34–46

Forbes B, Vlachopoulos N, Hyett AJ (2018) The application of distributed optical strain sensing to measure the strain distribution of ground support members. FACETS 3: 195–226

Freeman TJ (1978) The behaviour of fully-bonded rock bolts in the Kielder experimental tunnel. Tunnels and Tunnelling International 10(5): 37–40

Grasselli G (2005) 3D Behaviour of bolted rock joints: experimental and numerical study. International Journal of Rock Mechanics and Mining Sciences 42(2005): 13–24

Hoek E (2007) Rockbolts and cables. Practical Rock Engineering. https://www.rocscience.com/assets/resources/learning/hoek/Practical-Rock-Engineering-Full-Text.pdf Accessed 2024-12-12

Hoek E, Carranza-Torres C, Corkum B (2002) Hoek-Brown Failure Criterion – 2002 Edition. 5th North American Rock Mechanics Symposium, Toronto, ON, Canada, 2002, 1: 67-273

Hyett AJ, Moosavi M, Bawden WF (1996) Load distribution along fully grouted bolts, with emphasis on cable bolt reinforcement. Numerical and Analytical Methods in Geomechanics 20: 517–544

Li CC, Kristjansson G, Høien AH (2016) Critical embedment length and bond strength of fully encapsulated rebar rockbolts. Tunnelling and Underground Space Technology 59(2016): 16–23

Li CC, Stillborg B (1999) Analytical models for rock bolts. International Journal of Rock Mechanics and Mining Sciences 36(1999): 1013–29

Ren FF, Yang ZJ, Chen JF, Chen WW (2010) An analytical analysis of the full-range behaviour of grouted rockbolts based on a tri-linear bond-slip model. Construction and Building Materials 24: 361–370

Rocscience (n.d.) Bolt Support Models. https://www.rocscience.com/help/rs2/verification-theory/theory-manuals/bolts. Accessed 2024-12-12